



**HAL**  
open science

## HDO and H<sub>2</sub>O vertical distributions and isotopic ratio in the Venus mesosphere by Solar Occultation at Infrared spectrometer on board Venus Express

A. Fedorova, Oleg Korablev, A.-C. Vandaele, Jean-Loup Bertaux, D. Belyaev,  
A. Mahieux, E. Neefs, W.V. Wilquet, R. Drummond, Franck Montmessin, et  
al.

### ► To cite this version:

A. Fedorova, Oleg Korablev, A.-C. Vandaele, Jean-Loup Bertaux, D. Belyaev, et al.. HDO and H<sub>2</sub>O vertical distributions and isotopic ratio in the Venus mesosphere by Solar Occultation at Infrared spectrometer on board Venus Express. *Journal of Geophysical Research. Planets*, 2008, 113 (E5), pp.E00B22. 10.1029/2008JE003146 . hal-00349253

**HAL Id: hal-00349253**

**<https://hal.science/hal-00349253>**

Submitted on 9 Mar 2016

**HAL** is a multi-disciplinary open access archive for the deposit and dissemination of scientific research documents, whether they are published or not. The documents may come from teaching and research institutions in France or abroad, or from public or private research centers.

L'archive ouverte pluridisciplinaire **HAL**, est destinée au dépôt et à la diffusion de documents scientifiques de niveau recherche, publiés ou non, émanant des établissements d'enseignement et de recherche français ou étrangers, des laboratoires publics ou privés.

## HDO and H<sub>2</sub>O vertical distributions and isotopic ratio in the Venus mesosphere by Solar Occultation at Infrared spectrometer on board Venus Express

A. Fedorova,<sup>1</sup> O. Korablev,<sup>1</sup> A.-C. Vandaele,<sup>2</sup> J.-L. Bertaux,<sup>3,4</sup> D. Belyaev,<sup>1</sup> A. Mahieux,<sup>2</sup> E. Neefs,<sup>2</sup> W. V. Wilquet,<sup>2</sup> R. Drummond,<sup>2</sup> F. Montmessin,<sup>3,4</sup> and E. Villard<sup>3,4</sup>

Received 18 March 2008; revised 13 June 2008; accepted 26 August 2008; published 25 December 2008.

[1] Vertical distributions of the molecular density and mixing ratios of H<sub>2</sub>O and HDO in the Venus mesosphere have been obtained using Solar Occultation at Infrared (SOIR), a high-resolution (with  $\lambda/\delta\lambda \sim 20,000$ ) echelle spectrometer on Venus Express. The atmosphere is sounded in solar occultation in the range of altitudes from 65 to 130 km. Simultaneous measurements of water vapor lines in the spectral range around 2.61  $\mu\text{m}$  ( $3830 \text{ cm}^{-1}$ ) at altitudes between 70 and 110 km and HDO lines around 3.58  $\mu\text{m}$  ( $2715 \text{ cm}^{-1}$ ) at altitudes 70–95 km have been performed. During 1 1/2 years, from April 2006 to August 2007, 54 such measurements have been carried out at different locations of Venus from the north pole to middle south latitudes. Most of the observations at morning and evening terminator correspond to high northern latitudes. We report values of mixing ratio and isotopic ratio obtained for 22 of those measurements occurring in the northern polar area. The average value of the volume mixing ratio of H<sub>2</sub>O is  $1.16 \pm 0.24$  ppm and that of HDO is  $0.086 \pm 0.020$  ppm. A depletion in the mixing ratio for both H<sub>2</sub>O and HDO is observed at 85 km, which can be related to a depletion of CO<sub>2</sub> density above ( $\sim 95$  km) and a possible temperature inversion at these altitudes. The vertical variation of HDO and H<sub>2</sub>O mixing ratio is within a factor of 2–3 for the analyzed set of observations. The temporal variations have been investigated, and no noticeable variability of H<sub>2</sub>O is reported at high northern altitudes. The average ratio of HDO/H<sub>2</sub>O obtained in this work,  $240 \pm 25$  times the terrestrial ratio, is higher ( $\approx 1.5$  times) than the value of  $157 \pm 30$  times terrestrial reported for the lower atmosphere. This could be explained by a lower photodissociation of HDO and/or a lower escape rate of D atoms versus H atoms.

**Citation:** Fedorova, A., et al. (2008), HDO and H<sub>2</sub>O vertical distributions and isotopic ratio in the Venus mesosphere by Solar Occultation at Infrared spectrometer on board Venus Express, *J. Geophys. Res.*, *113*, E00B22, doi:10.1029/2008JE003146.

### 1. Introduction

[2] Venus' atmosphere is significantly drier than the atmosphere of the Earth: it contains from 1 to 100 ppm of water depending on altitude and location. As reviewed by *de Bergh et al.* [2006], the water vapor content measured below the cloud level is within 20–30 ppm, with much larger controversy at the cloud tops.

[3] Most of the H<sub>2</sub>O mesospheric observations were obtained from ground-based millimeter heterodyne spectroscopy [*Encrenaz et al.*, 1991, 1995; *Sandor and Clancy*, 2005]. Using the HDO line at 225.9 GHz and assuming a

D/H enrichment of 120 with respect to the terrestrial value, *Encrenaz et al.* [1991] obtained a mixing ratio of  $3.5 \pm 2.0$  ppm at 60–95 km. Later, observing the 187.31 GHz transition of H<sub>2</sub>O, *Encrenaz et al.* [1995] obtained 1 ppm above the clouds and 7 ppm (+5.0, –4.0) from the HDO line at 225.9 GHz, also assuming D/H = 120 terrestrial value. From a series of microwave observations, *Sandor and Clancy* [2005] reported a strong global variability of H<sub>2</sub>O on a 1–2 month time scale: at 65–100 km the mixing ratio ranged from  $0 \pm 0.06$  to  $3.5 \pm 0.3$  ppm. *Gurwell et al.* [2007] also reported an extreme variability of the Venus mesosphere dramatically demonstrated by submillimeter wave astronomy satellite (SWAS) observations from December 2002. Over the course of 5 days, a deep ground-state water absorption feature consistent with a water abundance of  $4.5 \pm 1.5$  ppm suddenly has transformed into a significantly shallower absorption, implying a decrease in the water abundance by a factor of 50 in less than 48 h.

<sup>1</sup>Space Research Institute, Moscow, Russia.

<sup>2</sup>Belgian Institute for Space Aeronomy, Brussels, Belgium.

<sup>3</sup>Service d'Aéronomie du CNRS, Verrières-le-Buisson, France.

<sup>4</sup>Also at Institut Pierre Simon Laplace, Université de Versailles Saint Quentin en Yvelines, Guyancourt, France.

[4] The isotopic ratio of HDO to H<sub>2</sub>O in standard mean ocean water (SMOW) equals  $3.1153 \times 10^{-4}$  and corresponds to  $([D]/[H])_{\text{smow}} = 1.5576 \times 10^{-4}$  [Hagemann *et al.*, 1970]. On Venus, first measurements of the D/H ratio were performed by the Pioneer Venus mass spectrometer LNMS in the low atmosphere (100 ( $\pm 12.5$ ) times terrestrial, corrected in 1997 to 157 ( $\pm 30$ ) times terrestrial) [Donahue *et al.*, 1982, 1997] and the ion mass spectrometer on the Pioneer Venus Orbiter at 155–160 km ( $[D^+]/[H^+] = (1.7 \pm 0.6) \times 10^{-2}$ ) or  $[D]/[H] = (2.2 \pm 0.6) \times 10^{-2}$ ) at the turbopause level of about 132 km [Hartle and Taylor, 1983]. These values have been confirmed later by ground-based observations in the 2.3  $\mu\text{m}$  nightside windows [de Bergh C. *et al.*, 1991]. Both in situ and remote-sensing determinations agree with one other and point to a strong deuterium enrichment in the Venus' atmosphere.

[5] In the near IR range above the clouds only one measurement of H<sub>2</sub>O and HDO has been reported [Bjoraker *et al.*, 1992]. High-resolution spectra were obtained between 2.59 and 2.65  $\mu\text{m}$  (3860–3770  $\text{cm}^{-1}$ ). A volume mixing ratio of H<sub>2</sub>O of  $2.09 \pm 0.15$  ppm at 72 km was reported and a D/H ratio of  $157 \pm 15$  times the value in the terrestrial ocean. Unfortunately, these results have never been published in any refereed literature.

[6] The enrichment of  $\sim 150$  of deuterium to hydrogen supports the idea of dramatic escape of water from Venus. Two scenarios are possible: either Venus has had at least 0.3% of the terrestrial ocean and lost its water during a catastrophic process, or Venus was dry from the beginning, and the present isotopic ratio is explained by cometary impacts, degassing, and escape processes. The unknown vertical distribution of H<sub>2</sub>O in the middle and upper atmosphere precludes accurate theoretical descriptions of the escape of D and H atoms. New measurements of HDO and H<sub>2</sub>O are necessary to understand the evolution of the Venusian climate.

[7] SOIR is a part of the SPICAV/SOIR experiment on the Venus Express spacecraft, operating on the orbit around Venus from April 2006 [Titov *et al.*, 2006]. It is a high-resolution IR spectrometer working in the range of 2.2–4.3  $\mu\text{m}$  [Bertaux *et al.*, 2007a; Nevejans *et al.*, 2006]. The experiment is dedicated to vertical sounding of the Venus' mesosphere in the range of 60–120 km by means of solar occultation. One of the main scientific goals of SOIR is a simultaneous measurement of H<sub>2</sub>O and HDO vertical profiles to retrieve the isotopic ratio in the mesosphere. The first results on water vapor measurements with SOIR have been reported by Bertaux *et al.* [2007b]. In this paper we present a new analysis of the observed H<sub>2</sub>O content, employing a better instrument calibration and using longer series of observations.

## 2. Measurements

### 2.1. Instrument Description

[8] Echelle spectrometer SOIR with an acoustooptic filtration of light is the first instrument with a spectral resolution above 20,000 orbiting another planet. It was first proposed for Venus Express mission by Korabiev and Bertaux [2002], and built at the Belgian Institute for Space Aeronomy in collaboration with a Belgian industry in a very short time.

[9] SOIR is designed to operate during solar occultations, when the instrument entrance optics is pointed toward the Sun as the latter goes down or up, allowing measurement of the atmospheric transmission of different layers of the atmosphere. The spectral range of SOIR from 2.32 to 4.25  $\mu\text{m}$  (2353–4310  $\text{cm}^{-1}$ ) allows measuring a number of atmospheric constituents showing up as absorbers in the transmission spectrum. High dispersion is provided by a 4 grooves  $\text{mm}^{-1}$ ,  $\arctan(2)$  incidence angle, echelle grating operating in diffraction orders from 101 (corresponding to the wavelengths of 4.4  $\mu\text{m}$ ) to 194 (2.3  $\mu\text{m}$ ). Each diffraction order covers a spectral interval from 20 to 40  $\text{cm}^{-1}$ . The diffraction orders are separated by an acoustooptic tunable filter (AOTF). In the AOTF the radiation is filtered owing to volume diffraction on the acoustooptic wave excited within a birefringent crystal by a piezoelectric transducer at high frequency (RF = 14–26 MHz). The diffracted light is then analyzed by the echelle spectrometer. The central wavelength of the AOTF band-pass function is determined for the RF applied from the frequency-wavelength calibration as described by Mahieux *et al.* [2008]. The full width at half maximum FWHM of the AOTF band pass is around 24  $\text{cm}^{-1}$ , and the profile of the AOTF band-pass function is close to a  $(\sin x/x)^2$  function with a number of significant side lobes. As a result, spectral features leaking from several adjacent diffraction orders contribute to the spectrum observed on the detector with different weights that will be discussed in section 3.

[10] The SOIR detector (from SOFRADIR) has 320 columns oriented along the spectral dispersion (wavelengths) and 256 rows along the spectrometer's slit (spatial dimension). To avoid saturation, short integration times are used (20 to 30 ms), depending on the wavelength at which the measurement is taken. The background signal (Dark Current + Thermal emission of optics) is measured and subtracted onboard. In order to improve the signal-to-noise ratio (SNR), a number of measurements can be accumulated as long as the total measuring time remains below 250 ms.

[11] The slit height is 30 arc min, and it is projected onto 32 rows of the detector. The slit width is equivalent to two detector pixels in the spectral direction. The spectral resolution of the spectrometer is very high and equals  $\sim 0.13$   $\text{cm}^{-1}$  at 2500  $\text{cm}^{-1}$  (order 111) and  $0.27$   $\text{cm}^{-1}$  at 4300  $\text{cm}^{-1}$  (order 192). The corresponding resolving power  $[\lambda/\Delta\lambda = \nu/\Delta\nu]$  is  $\sim 20,000$  [Mahieux *et al.*, 2008].

[12] Owing to telemetry limitations, only eight spectra, each of 320 pixels long can be downloaded per second. During most of observations on Venus orbit, these eight spectra are taken in four different diffraction orders (different tunings of the AOTF), each corresponding to two large bins of 16 or 12 rows on the detector.

[13] The detailed description of the instrument can be found by Nevejans *et al.* [2006] and Bertaux *et al.* [2007a]. Calibrations and in-flight performances of the instrument, including data handling, on board background subtraction, calibrations of the AOTF and the echelle spectrometer are described in detail by Mahieux *et al.* [2008].

### 2.2. Observations

[14] For accurate measurements of the isotopic ratio, simultaneous observations of H<sub>2</sub>O and HDO absorption lines are required. As discussed above, only four 20–30  $\text{cm}^{-1}$

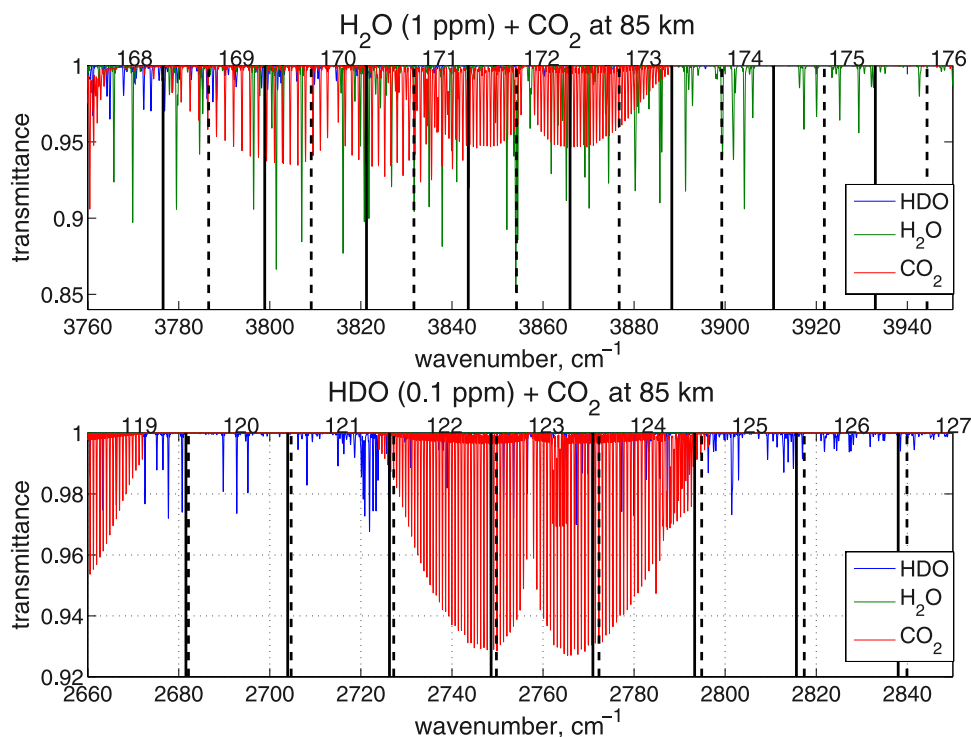


**Figure 1.** Synthetic spectra of H<sub>2</sub>O (green), HDO (blue), and CO<sub>2</sub> (red) at the target altitude of 85 km in solar occultation geometry. The top corresponds to the spectral interval 3760–3940 cm<sup>-1</sup> (2.6 μm) dedicated to H<sub>2</sub>O measurements; the bottom shows the spectral interval 2660–2840 cm<sup>-1</sup> (3.6 μm) dedicated to HDO measurements. Order boundaries are shown as solid (beginning) and dashed (end) black lines. The numbers above each plot show the order number and are located at the center of the order. Orders 171 and 121 are used mainly for retrieval of H<sub>2</sub>O and HDO abundance, respectively.

portions of the spectrum within the spectral range of SOIR (four diffraction orders) can be acquired during a single occultation. We therefore carefully chose the spectral range for H<sub>2</sub>O and HDO detection attributing at least one order for HDO and another one for H<sub>2</sub>O. The priority was given to spectral ranges with strong lines of the gases of interest, and minimal contamination from other gases. There are several strong transitions of H<sub>2</sub>O within the spectral range of SOIR. The most preferable for the H<sub>2</sub>O retrieval is the strongest 3600–3900 cm<sup>-1</sup> band, which includes lines of  $\nu_1$  and  $\nu_3$  fundamental transitions. Below 3750 cm<sup>-1</sup> a strong CO<sub>2</sub> 2.7 μm band prevents the accurate determination of H<sub>2</sub>O, being completely saturated below 85 km of tangent altitude in solar occultation geometry.

[15] For HDO we can consider the two strongest transitions within SOIR spectral range: the fundamental bands  $\nu_3$  (001–000) near 3707 cm<sup>-1</sup> (2.69 μm) and  $\nu_1$  (100–000) near 2723 cm<sup>-1</sup> (3.67 μm). The first one is blended by the 2.56 μm band of the main H<sub>2</sub>O isotope, and the HDO transitions are weak. The best candidate is the strong fundamental HDO band  $\nu_1$  (100–000), completely isolated from H<sub>2</sub>O transitions. Moreover, this spectral range is free from detectable CO<sub>2</sub> lines. Considering the other molecules, HCl lines are also located in the range of 3.67 μm. But these lines are isolated and do not contaminate HDO lines.

[16] Synthetic spectra of Venus atmosphere limb transmission expected at the tangent altitude of 90 km, showing separately H<sub>2</sub>O and HDO lines, and all isotopologues of CO<sub>2</sub> are presented in Figure 1 for the selected ranges

discussed above. The diffraction orders of SOIR are indicated. The orders numbers from 170 to 172 and 174 have been used for H<sub>2</sub>O measurements. Most of the observations so far have been performed in the order 171. The strongest lines of H<sub>2</sub>O in this range correspond to the rotational structures of (001)–(000) transition. For the retrieval of the HDO density, the orders 121 and 125 have been chosen, most of the observations having been performed in the order 121.

### 2.3. Observation Coverage

[17] We have considered the operations from April 2006 to August 2007. During this period 54 orbits have been dedicated specifically to simultaneous measurements of H<sub>2</sub>O and HDO in the Venus' mesosphere. Among them, on 47 orbits an additional spectral range dedicated to CO<sub>2</sub> was scanned simultaneously in order to measure independently the atmospheric density profile and to reduce spacecraft pointing uncertainties. We address an interested reader to the paper by *Vandaele et al.* [2008, Figure 1] for the illustration of transmission evolution during an occultation in these diffraction orders. Vandaele et al.'s Figure 1 gives an example of the evolution of one occultation (sunset 15 April 2007) in the order 121, 171, 149, and 190. It is a typical observation dedicated to H<sub>2</sub>O, HDO, and CO measurements. Order 149 has been chosen for CO<sub>2</sub> retrieval in the range of 3330–3357 cm<sup>-1</sup> where strong P and Q branches of 21102–00001 transition allow the measurement of the atmospheric density at the altitudes of 70–120 km.

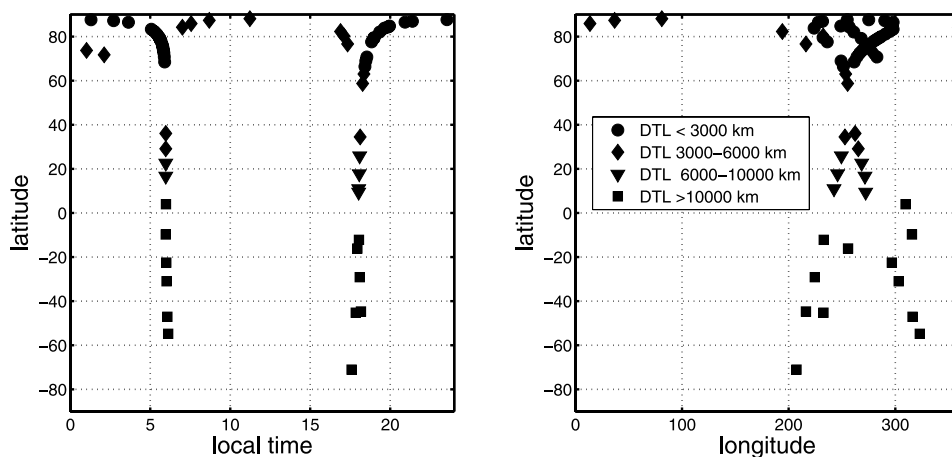


**Figure 2.** Spatial coverage for the simultaneous measurements of H<sub>2</sub>O and HDO. The maps of longitude versus latitude and local time versus latitude are presented. Most of the observations are located at high northern latitudes, corresponding to low distances from spacecraft to the limb. It reflects the peculiarity of the Venus Express polar orbit with the pericenter near the north pole.

[18] The list of the main CO<sub>2</sub> bands used for retrieval of atmospheric density is presented by *Vandaele et al.* [2008, Table 1]. In case of H<sub>2</sub>O and HDO, for the retrieval of the CO<sub>2</sub> density several orders (depending on the orbit) have been chosen: 111, 112 (isotope O<sup>16</sup>C<sup>12</sup>O<sup>18</sup>, spectral range 2470–2520 cm<sup>-1</sup>), 123 (spectral range 2748–2773 cm<sup>-1</sup>) and 148, and 149 (a transition 21102 – 00001 at 3285–3360 cm<sup>-1</sup>).

[19] The geographical distribution of observations for which H<sub>2</sub>O and HDO were measured simultaneously, and the dependence on local time are presented in Figure 2.

[20] Venus Express spacecraft is on highly elongated orbit with a pericenter located at about 250 km near the north pole, and an apocenter at 65000 km above the southern hemisphere of Venus [*Titov et al.*, 2006]. From such an orbit, most of the solar occultations are observed at high northern latitudes with smaller distance to limb (near the pericenter), another part corresponding to relatively large distances to the limb and low latitudes. The vertical resolution of the occultation depends directly on the distance to the limb. The attitude of the spacecraft is maintained so that the slit of SOIR would be nearly parallel to the limb at 65 km. Near the pericenter the vertical resolution is generally better than 1.5 km. But because of the rotation of the slit with respect to the limb during one occultation and as the distance to limb is changing with the spacecraft motion, the vertical resolution during one observation usually varies from several hundred meters to several kilometers. This effect is described in detail in the paper of *Vandaele et al.* [2008, section 3]. In the present study we have considered only the measurements taken near the pericenter with small distances to the limb in order to minimize uncertainties. About 35 H<sub>2</sub>O measurements have been performed near the pericenter with the distance to the limb below 6000 km. All of them are located close to the north pole. We have further constrained the analyzed set to identical spectral ranges. We concentrated on orbits where the orders numbers 171 and 121 have been used for H<sub>2</sub>O and HDO respectively. In all, 22 orbits have been analyzed. The list of reported observations including universal time, latitude, longitude, local time, and distance to the limb at the altitude of 80 km is presented in Table 1. Within the considered set of observations which includes both sunrises

and sunsets, latitudes vary from 60° to 86° N, and the local time is 5–6 h and 17–19 h.

### 3. Retrieval Process

[21] In solar occultation the transmission spectrum is directly obtained from relative measurements, and the photometric calibration of the instrument is generally not required. The processing of raw SOIR data, including nonlinearity and other corrections up to the construction of transmission spectra, and spectral calibration is described by *Mahieux et al.* [2008]. The reference spectrum is obtained as a weighted average of solar spectra recorded outside of the atmosphere (at the altitudes from 160 to 200 km) [*Vandaele et al.*, 2008]. A forward model of gas absorption and the retrieval of vertical profiles of atmospheric constituents based on “onion-peeling” method are described in detail by *Vandaele et al.* [2008]. In the present paper we discuss only the details related specifically to H<sub>2</sub>O and HDO spectroscopy.

#### 3.1. Spectroscopic Data

[22] As a basis, the HITRAN 2004 database [*Rothman et al.*, 2005] with the update of 2006 for H<sub>2</sub>O has been used. Nevertheless, no significant modification in the spectral range of interest was found in the 2006 update. Among the spectroscopic data like line strengths and positions, temperature coefficients and pressure shifts, HITRAN database contains line widths for air and self broadening. The widths of spectral lines broadened by CO<sub>2</sub> which is the main component of the Venus’ atmosphere (96.3%) are not well known. The first measurements of CO<sub>2</sub> broadening for H<sub>2</sub>O lines have been done by *Howard et al.* [1956a, 1956b, 1956c, 1956d]. This work recommended a constant factor of 1.3 to translate from the air to CO<sub>2</sub> broadening. This factor has been then widely used in the 1990s for investigation of the Venus’ atmosphere [*Pollack et al.*, 1993]. Later accurate laboratory measurements of CO<sub>2</sub> broadening in the near-infrared range were made by *Gamache et al.* [1995]. The authors compared their laboratory measurements of CO<sub>2</sub>-broadened half widths with some recent experimental work and theoretical calcu-

**Table 1.** Venus Express Orbits During Which Simultaneous Observations of H<sub>2</sub>O, HDO, and CO<sub>2</sub> Have Been Performed With Low Distances to the Limb, Near the Pericenter of an Orbit<sup>a</sup>

Orbit	Date	Obs	Longitude	Latitude	LT	Ls	DTL	O1	O2	O3	O4	H <sub>2</sub> O-1 (ppm)	H <sub>2</sub> O-2 (ppm)	HDO <sup>b</sup> (ppm)
244	21 Dec 2006	IN	248.91	84.80	19.96	63.08	2160.52	121	171	111	112	1.08 ± 0.10	1.24 ± 0.13	0.097 ± 0.010
247	24 Dec 2006	IN	256.82	84.39	19.88	67.82	1558.68	121	171	149	192	1.38 ± 0.13	1.36 ± 0.17	0.098 ± 0.012
251	28 Dec 2006	IN	261.13	82.09	19.34	74.14	1627.02	121	171	112	181	1.00 ± 0.10	1.28 ± 0.05	0.092 ± 0.004
255	1 Jan 2007	IN	268.06	79.19	18.99	80.46	1729.67	121	171	148	191	0.89 ± 0.05	1.03 ± 0.05	0.081 ± 0.003
262	8 Jan 2007	IN	282.80	70.76	18.54	91.52	2111.65	121	171	111	133	1.02 ± 0.06	1.08 ± 0.07	0.086 ± 0.004
345	1 Apr 2007	E	13.69	85.93	7.56	224.28	3315.49	121	171	149	133	0.84 ± 0.06	0.68 ± 0.06	0.056 ± 0.007
347	3 Apr 2007	E	36.86	87.34	8.69	227.52	3293.40	121	171	149	133	0.84 ± 0.04	0.74 ± 0.04	0.070 ± 0.014
349	5 Apr 2007	E	81.05	88.13	11.23	230.76	3281.31	121	171	149	190	0.80 ± 0.05	0.63 ± 0.04	0.054 ± 0.006
358	14 Apr 2007	E	194.10	82.30	16.90	245.36	3434.61	121	171	149	133	0.75 ± 0.05	0.64 ± 0.05	0.057 ± 0.011
434	29 Jun 2007	IN	264.07	70.83	5.88	7.99	2060.91	121	171	111	125	1.28 ± 0.11	1.15 ± 0.12	0.075 ± 0.011
435	30 Jun 2007	IN	266.74	72.54	5.85	9.59	1980.57	121	171	112	190	1.14 ± 0.03	1.21 ± 0.03	0.084 ± 0.002
438	3 Jul 2007	IN	274.52	76.11	5.76	14.36	1848.39	121	171	149	132	1.54 ± 0.10	1.50 ± 0.15	0.106 ± 0.010
440	5 Jul 2007	IN	279.49	77.84	5.68	17.54	1805.21	121	171	118	151	0.96 ± 0.09	1.25 ± 0.05	0.084 ± 0.003
442	7 Jul 2007	IN	284.24	79.30	5.59	20.72	1777.70	121	171	149	184	1.47 ± 0.05	1.35 ± 0.07	0.091 ± 0.005
443	8 Jul 2007	IN	286.51	79.97	5.53	22.31	1768.19	121	171	111	188	1.22 ± 0.07	1.20 ± 0.07	0.087 ± 0.004
445	10 Jul 2007	IN	290.81	81.18	5.41	25.49	1758.40	121	171	149	130	1.66 ± 0.10	1.53 ± 0.14	0.106 ± 0.010
447	12 Jul 2007	IN	294.66	82.31	5.26	28.67	1751.90	121	171	111	136	1.22 ± 0.05	1.22 ± 0.04	0.088 ± 0.006
456	21 Jul 2007	IN	298.02	86.52	3.64	42.93	1780.27	121	171	112	145	1.24 ± 0.04	1.26 ± 0.02	0.086 ± 0.003
462	27 Jul 2007	IN	254.94	87.68	23.55	52.39	1833.11	121	171	149	180	1.60 ± 0.09	1.59 ± 0.13	0.106 ± 0.011
471	5 Aug 2007	IN	232.25	79.49	18.98	76.02	2088.11	121	172	123	180	0.94 ± 0.12	1.36 ± 0.04	0.118 ± 0.004
486	20 Aug 2007	IN	251.33	66.41	18.42	90.16	2766.10	121	171	149	190	1.54 ± 0.10	1.31 ± 0.18	0.081 ± 0.006
487	21 Aug 2007	IN	253.47	63.01	18.36	91.78	3001.76	121	171	149	190	1.11 ± 0.05	0.99 ± 0.05	0.079 ± 0.005

<sup>a</sup>Latitude, longitude, and local time are given for the altitude of 80 km. Obs can be sunrise as E or sunset as IN; LT is the local time on Venus in Venusian hours; Ls is the solar longitude; DTL is the distance to the limb in km; O1, O2, O3, and O4 are the number of orders observed during the orbit; H<sub>2</sub>O-1 is the H<sub>2</sub>O mixing ratio in ppm averaged for altitudes between 75 and 112 km; H<sub>2</sub>O-2 is the H<sub>2</sub>O mixing ratio in ppm averaged for altitudes between 75 and 95 km; and HDO is the HDO mixing ratio in ppm averaged for altitudes between 75 and 95 km.

lations, and investigated the resulting temperature dependence of the half widths. The scaling factor from air broadening varies from 1.3 to 2.0, depending on a particular transition. Recently, *Brown et al.* [2007] published the CO<sub>2</sub>-broadened water parameters (half width, line shift, and temperature dependence of the widths) for the transitions between 200 and 900 cm<sup>-1</sup>. They obtained ratios of CO<sub>2</sub>-broadened to N<sub>2</sub>-broadened widths which varied widely from 0.95 to 3.07 with an average ratio of 1.67. To account for the CO<sub>2</sub> broadening of lines in the Venusian atmosphere, we have multiplied the air-broadened half widths from the HITRAN 2004 database by 1.7 [*Gamache et al.*, 1995; *Brown et al.*, 2007]. The HDO line strengths in the HITRAN are scaled to the isotopic ratio of HDO to H<sub>2</sub>O in standard mean ocean water (SMOW) ( $3.1115 \times 10^{-4}$ ).

### 3.2. Forward Modeling of H<sub>2</sub>O and HDO Transmittance Spectra

[23] Using the forward model [*Vandaele et al.*, 2008], the synthetic spectra of water vapor and HDO are calculated for the geometry of the solar occultation. Figures 3 and 4 illustrate the synthetic models for HDO in the order 121 (2703–2727 cm<sup>-1</sup>) and for H<sub>2</sub>O in the order 171 (3823–3853 cm<sup>-1</sup>) at a tangential altitude of 90 km. CO<sub>2</sub> absorption lines have also been considered in those simulations. Atmospheric temperature and pressure profiles were taken from the Venus International Reference Atmosphere (VIRA) [*Keating et al.*, 1985] for the dayside. H<sub>2</sub>O and HDO are assumed uniformly mixed with the volume mixing ratio of 1 ppm and 100 ppb, respectively. Monochromatic spectra have been converted to SOIR spectral resolution. Figures 3 and 4 (top) show modeling of gaseous absorption in “clear” case assuming there is no order mixing on detector.

[24] The contribution of adjacent diffraction orders complicates the spectra measured by SOIR with respect to the

synthetic model shown in Figures 3 and 4 (top). The mixing of diffraction orders occurs owing to a wider than specified AOTF band-pass function (FWHM of 25 cm<sup>-1</sup>), and the side lobes of this function (see discussion in the section 3.1 of *Vandaele et al.* [2008]). Figure 5 clearly demonstrates the contribution of different orders (actually ±3 orders) around the main order 121. Moreover, as described by *Mahieux et al.* [2008], the shape of the AOTF band-pass function is different for the beams coming from different parts of the spectrometer’s slit. As a result the contribution of adjacent orders is different for bins 1 and 2 recorded simultaneously during an observation (see section 2.1), where bin 1 and bin 2 correspond to the top and bottom parts of the slit.

[25] We reconstruct SOIR spectra in the 121 and 171 diffraction orders for bins 1 and 2 taking into account the overlapping of three orders from each side in Figures 3 and 4 (middle and bottom). In all, the seven diffraction orders contribute into the shown transmission spectra (from -3 to +3).

[26] With the mixing of orders the 121 diffraction order, which is originally free from CO<sub>2</sub> lines, becomes contaminated by CO<sub>2</sub> lines coming from adjacent orders 122–123 (compare Figure 1). This emphasizes the need of high accurate AOTF function taken into account more orders.

[27] The mixing of diffraction orders becomes even more important in the order 171 (2.6 μm) located close to a strong 2.7 μm CO<sub>2</sub> band. In Figure 5 we compare the synthetic model assuming the contribution of three diffraction orders from each side (Figure 5a) with a model assuming contribution of six orders (Figure 5b) with SOIR spectrum from the orbit 462 recorded at the altitude of 107 km. At this altitude the signal is not decreased by aerosol extinction, and the signal-to-noise of SOIR for order 171 between 100 and 290 pixels is better than 1000. It allows detecting very weak absorption features with a relative depth below 0.1–

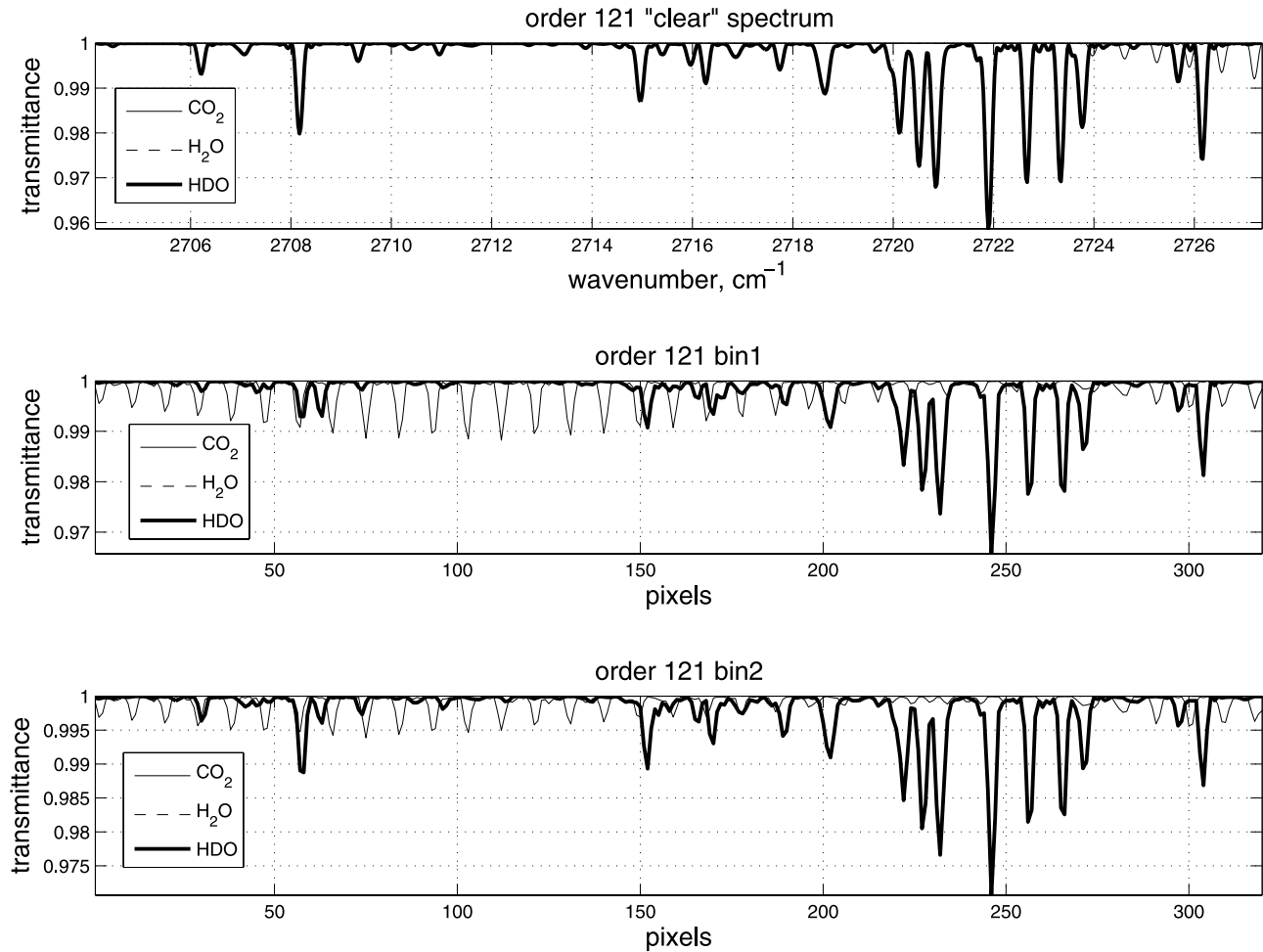


**Figure 3.** Synthetic models of HDO and CO<sub>2</sub> in the order 121 (2703–2727 cm<sup>-1</sup>). Frequency preset on the acoustooptic tunable filter (AOTF) is 15822.62 kHz. Solar occultation geometry is considered with the tangential altitude of 90 km. The VIRA atmospheric model was used. Volume mixing ratio of HDO was assumed to be equal to 100 ppb. Monochromatic spectra have been converted to SOIR resolution. The thick solid line corresponds to HDO, and the thin solid line corresponds to CO<sub>2</sub>. H<sub>2</sub>O lines are also taken into account (dashed thin line) but are weak in this range. Top shows a “clear” spectrum of gaseous absorption in the range of 2703–2727 cm<sup>-1</sup> without any order mixing. Middle shows a synthetic spectrum taking into account the mixing of 7 orders (from -3 to +3) for bin 1 (spectra obtained in the bottom part of the slit). Bottom shows a synthetic spectrum taking into account the mixing of 7 orders (from -3 to +3) for bin 2 (spectra obtained in the top part of the slit). The different calibration of frequency-wavelength functions for different bins (or rows on the matrix) introduces differences in the spectra which correspond to different rows of the detector.

0.2%. Figure 5 demonstrates that the structures in order 171 are not a noise but CO<sub>2</sub> lines coming from the orders 165 to 167. These orders correspond to the third side lobe of the AOTF function which has an amplitude of only 1% of the central lobe. However, the strong absorption in the CO<sub>2</sub> 2.7 μm band (up to 50%) results in a quasi-chaotic structure with relative depths of 0.1–0.3% inside the order 171, contaminating the measured H<sub>2</sub>O spectrum.

[28] Although the AOTF band pass function is not well constrained for such distant side lobes, taking into account six adjacent orders allows to reduce the residual error. We therefore take into consideration the contribution from ±6 orders in all further modeling of H<sub>2</sub>O and HDO spectra in orders 121 and 171.

### 3.3. Fitting

[29] The local densities of considered molecules (CO<sub>2</sub>, HDO, and H<sub>2</sub>O) are retrieved using the traditional onion-peeling method [e.g., Rodgers, 2000]. The main idea of this method in application to SOIR data is described by Vandaele *et al.* [2008] (see section 3.3 and Figure 4). The local densities of molecules are retrieved from the top of the atmosphere downward. The retrieved quantities are used for simulating the spectra corresponding to the lower layers. To calculate the absorption cross sections of the selected molecules, the atmospheric temperature-pressure profile was taken from VIRA [Keating *et al.*, 1985].

[30] The measured spectra are fitted to the model using minimization of  $\chi^2$  and the simplex algorithm [Press *et al.*, 1992] with two variables: local density of molecules (H<sub>2</sub>O,

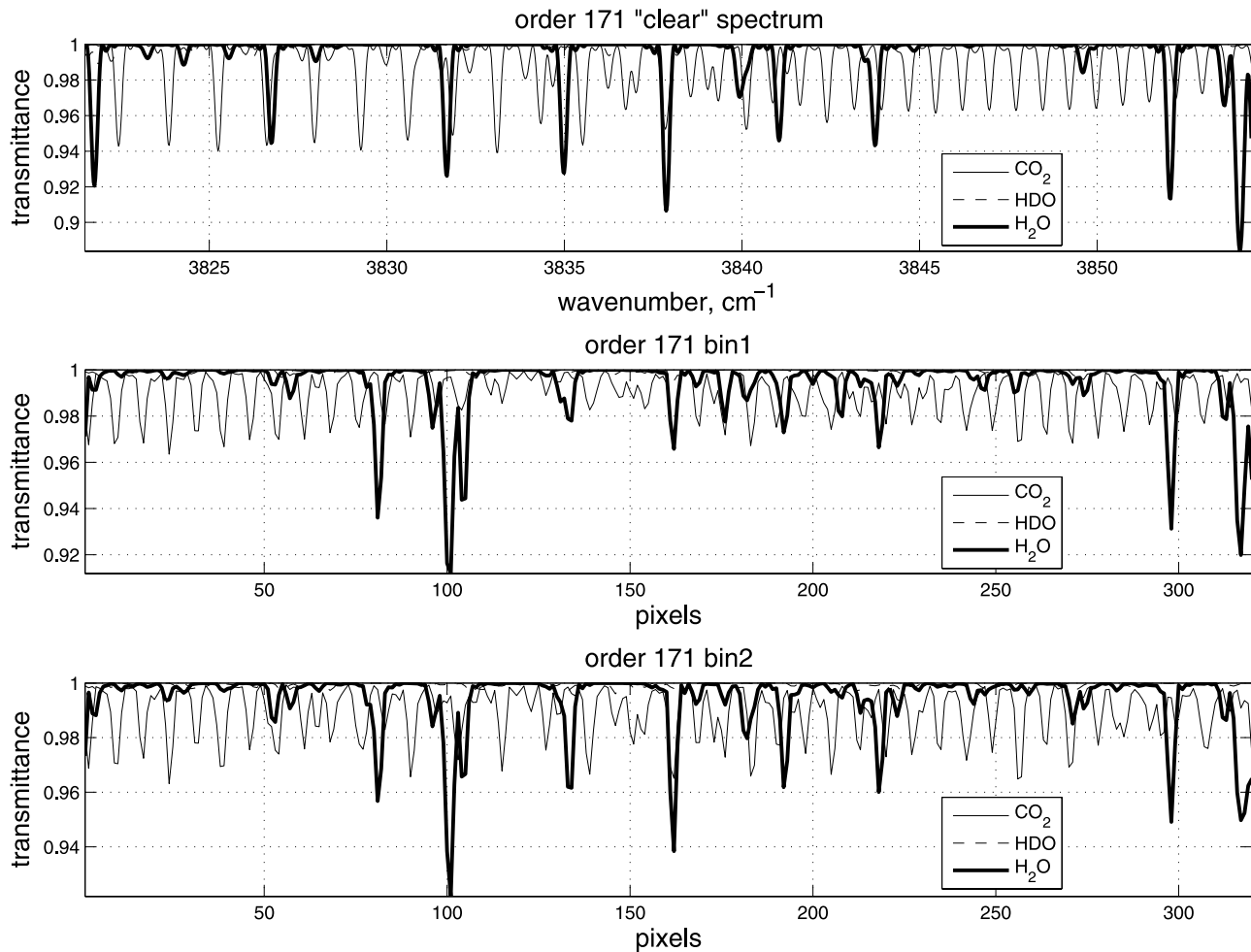


**Figure 4.** Synthetic models of H<sub>2</sub>O and CO<sub>2</sub> in the order 171 (3823–3853 cm<sup>-1</sup>). The frequency preset on the AOTF is 22946.44 kHz. Solar occultation geometry is considered with the tangential altitude of 90 km. VIRA atmospheric model was used. Volume mixing ratios of H<sub>2</sub>O were assumed to be equal to 1 ppm. Monochromatic spectra have been converted to the SOIR resolution. The thick solid line corresponds to H<sub>2</sub>O, and the thin solid line corresponds to CO<sub>2</sub>. HDO lines are also taken into account (dashed thin line) but are weak in this range. The presentation of different top, middle, and bottom is the same as for Figure 3.

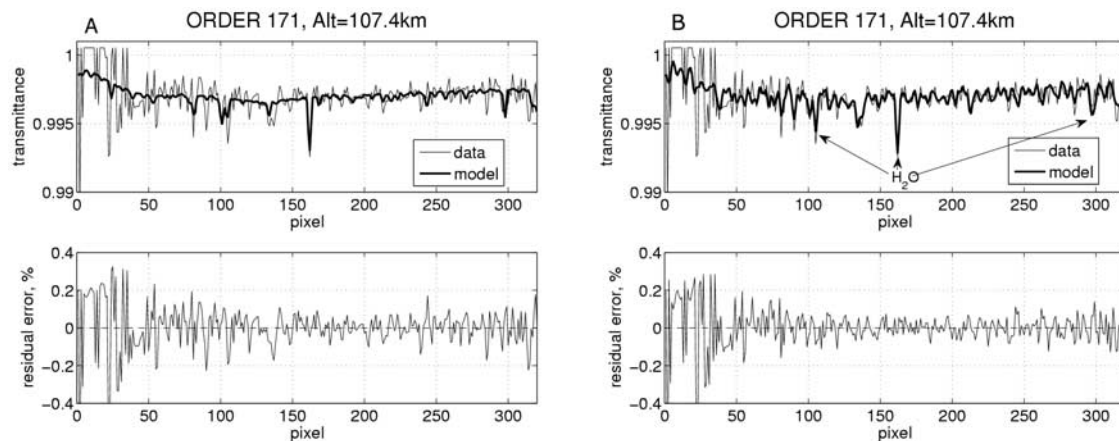


**Figure 5.** Contamination of adjacent orders in the main order 171 used for H<sub>2</sub>O retrieval. (a)  $\pm 3$  orders around the main order have been taken into account. (b)  $\pm 6$  orders around the main order have been taken into account. Those data were obtained during orbit 462 (27.07.2007) at the location latitude 87°N, longitude 245°E, 23.55 h Venusian local time (LT), distance to the limb 1830 km.

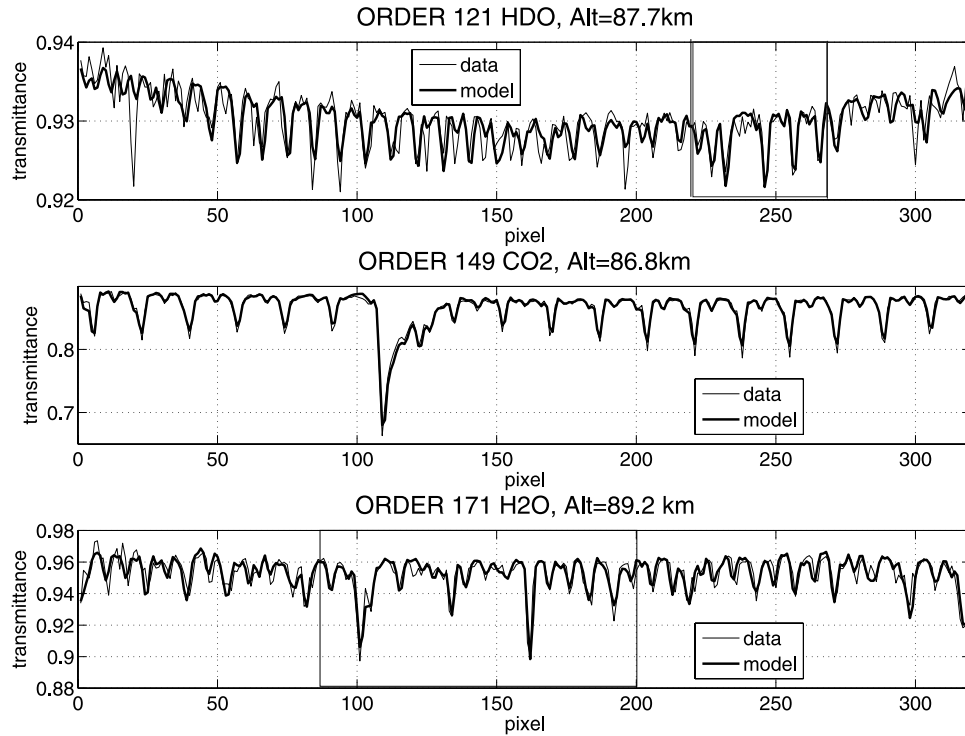


**Figure 6.** Examples of data fitting for three orders 121 (HDO), 149 (CO<sub>2</sub>), and 171 (H<sub>2</sub>O) at the altitudes 86–89 km. Those data were obtained during orbit 462 (27.07.2007) at the location latitude 87°N, longitude 245°E, 23.55 h LT, distance to the limb 1800 km. The light boxes relate to the spectral range chosen for HDO and H<sub>2</sub>O retrieval.

HDO, or CO<sub>2</sub>) and aerosol extinction that determines the continuum level of the transmittance spectrum. The best density value for every measurement is retrieved automatically, minimizing  $\chi^2$  statistically weighted according to the uncertainties of the measured quantity:

$$\chi^2 = \sum_{p1}^{p320} (T_{data}(i) - T_{model}(i))^2 / \sigma(i)^2$$

where  $T_{data}(i)$  and  $T_{model}(i)$  are the measured and modeled spectrum of transmittance for pixel  $i$ .  $\sigma(i)$  is the statistical error determined from the signal-to-noise of the measured spectra which vary depending on diffraction order and detector pixel. Examples of the best fit spectra for H<sub>2</sub>O, HDO, and CO<sub>2</sub> are presented in Figure 6. The light gray boxes in the top and bottom indicate the spectral range chosen for the retrieval of H<sub>2</sub>O and HDO density. The preference has been given to the lines with higher intensity, lower sensitivity to temperature, which are less contaminated with CO<sub>2</sub> lines. Some lines appear broader in the model than in the observed spectrum that could be explained by the uncertainty of the assumed temperature profile (as partially described by *Vandaele et al.* [2008]), and possibly by sampling on the detector's pixels. For the retrieval we used several lines that minimize the discrepancy in the line widths, as described in more detail in section 3.4. The curvature of measured spectrum in Figure 6 (top) is due to undercorrection of detector's nonlinearity apparent at the edges of order's spectral range. Figure 7 demonstrates a typical result of the retrieval of the gaseous densities for one

selected orbit, showing the simultaneous vertical distributions of the local densities for HDO, H<sub>2</sub>O, and CO<sub>2</sub>.

### 3.4. Uncertainty of Results

[31] There are several sources of uncertainties in our results: spectroscopic data set (in particular the broadening factor for H<sub>2</sub>O in the CO<sub>2</sub> atmosphere), atmospheric data set and assumed temperature-pressure profiles, and instrumental calibration uncertainties. The calibration uncertainties include AOTF frequency-wavelength calibration that determines the position of the maximum of the AOTF function versus the preset frequency for bin 1 and bin 2. This has been obtained with a precision of 0.83 cm<sup>-1</sup> [*Mahieux et al.*, 2008]. Uncertainties on the shape of the AOTF function, including the contribution of the side lobes are still poorly estimated. Detailed sensitivity analysis on this parameter will be performed in the near future.

[32] The uncertainties due to a shift of the maximum of the AOTF function of 1 cm<sup>-1</sup> give an error of ~8% on the retrieved values at altitude from 70 to 95 km for HDO and 7% for H<sub>2</sub>O. The uncertainties due to the shape of the AOTF function (the cutoff of the far wing in  $\pm 3$  orders during the retrieval that corresponds to removal of the contribution of the far side lobes) is the most important for H<sub>2</sub>O retrieval and put the error to 4% at the altitude from 70 to 100 km, which increases up to 40% at the altitude of 110 km. For HDO uncertainties from order mixing are below than 4%.

[33] The uncertainties coming from the assumed spectral instrument function of the echelle spectrometer also give

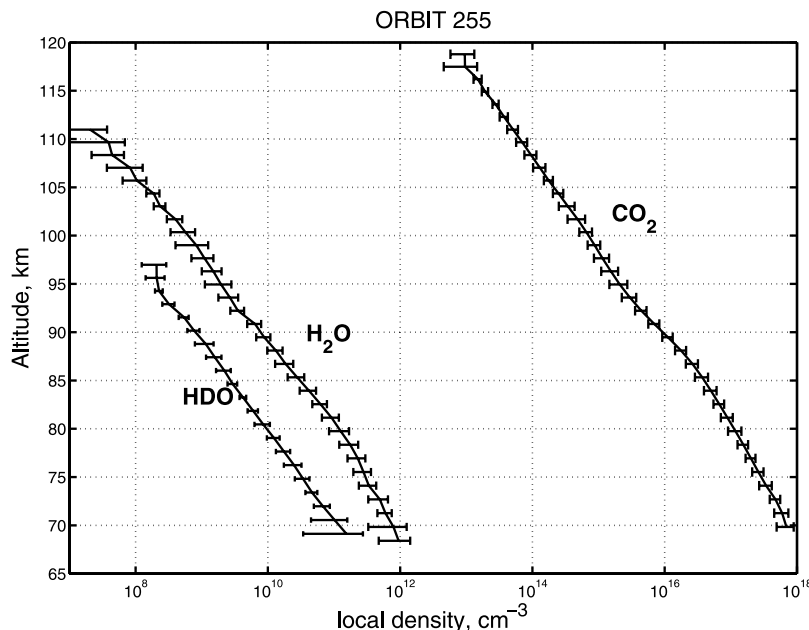


**Figure 7.** Example of retrieved densities of HDO, H<sub>2</sub>O, and CO<sub>2</sub> in molecules cm<sup>-3</sup> for orbit 255 corresponding to the northern latitude 79.2°, longitude 261°E, and 19 h LT and distance to the limb 1730 km at altitude 80 km.

rise to some systematic bias in the result. The sensitivity to variation of the instrument spectral function half width was investigated for each molecule. A variation of the half width by 20% results on average 8.5% of error in gaseous density, slightly varying with altitude and diffraction order. For different orders the widths of this function varies from 0.16 cm<sup>-1</sup> for the order 121 to 0.22 cm<sup>-1</sup> for the order 171 that may also bias the relation between different species detected in distant orders.

[34] The comparison of results obtained for bin 1 and bin 2 also can provide a good estimation of uncertainties. For HDO (order 121) the total uncertainty on the average amounts to 8–14% and varies a little with altitude and from orbit to orbit that could be explained by different calibrations for these spectra and rotation of slit with respect to the limb.

[35] Uncertainties on spacecraft pointing and in fact the unknown real pressure and temperature at the location of measurements add systematic biases to the retrieval. To account for this, we should use CO<sub>2</sub> density retrieved from CO<sub>2</sub> lines during the same observation as presented in Figure 7. The absorption cross sections of the molecules are sensitive to temperature and pressure. In particular, the line strengths depend on the temperature and the power of dependence is determined by the energy of transition (see equation 6 by *Vandaele et al.* [2008]). As already mentioned, in the case of H<sub>2</sub>O and HDO retrieval, CO<sub>2</sub> density is retrieved from several different orders: 111, 112, 123, 148, and 149. The line strengths inside these ranges are not very sensitive to temperature variations. The intensity of the H<sub>2</sub>O and HDO lines are also not very sensitive to temperature, no more than 50% increase for a variation of temperature of 100 K. The uncertainties on temperature can be estimated by comparing the retrievals obtained with two different temperature profiles (Figure 8). We have chosen an extreme case that is assuming a deep inversion of temperature at the altitudes between 85 and 95 km. Retrievals of CO<sub>2</sub> (order

149, top) and H<sub>2</sub>O (order 171, bottom) obtained for orbit 462 are presented in Figure 8. Left shows the temperature profiles used for the retrievals, middle shows the retrieved densities, and right shows the relative difference in % calculated as

$$\frac{N_1(z) - N_2(z)}{N_1(z)}$$

where  $N_1(z)$  and  $N_2(z)$  are the local densities for the first and second temperature profiles. For H<sub>2</sub>O, variations due to temperature are not very high and do not exceed 10%. For CO<sub>2</sub>, depending on the order, the error can reach 20% at the altitudes of the inversion (85–100 km).

[36] The importance of the retrieved density profiles for the determination of the volume mixing ratios of the minor species is shown in Figure 9. Mixing ratios of H<sub>2</sub>O from orbit 442 obtained by division by the model density from VIRA or by the CO<sub>2</sub> density retrieved in this work are compared.

#### 4. Results

[37] We report here results for 22 orbits obtained from January 2006 to August 2007. All the orbits have been performed at the latitudes of 63°–88°N on morning and evening terminators with the distance to limb below 3500 km.

[38] To detect variability of HDO and H<sub>2</sub>O abundance with time, several sets of observations have been done. In the present analysis the following sets are considered: 5 orbits from 244 to 262 at December 2006 to January 2007, 4 orbits from 345 to 358 at April 2007, and 15 orbits from 434 to 487 at June–August 2007. Figure 10 demonstrates the density retrieved for 5 consecutive orbits from 244 to 262 and 3 orbits from 442 to 445 obtained close to the north pole. No strong variations of the H<sub>2</sub>O and HDO

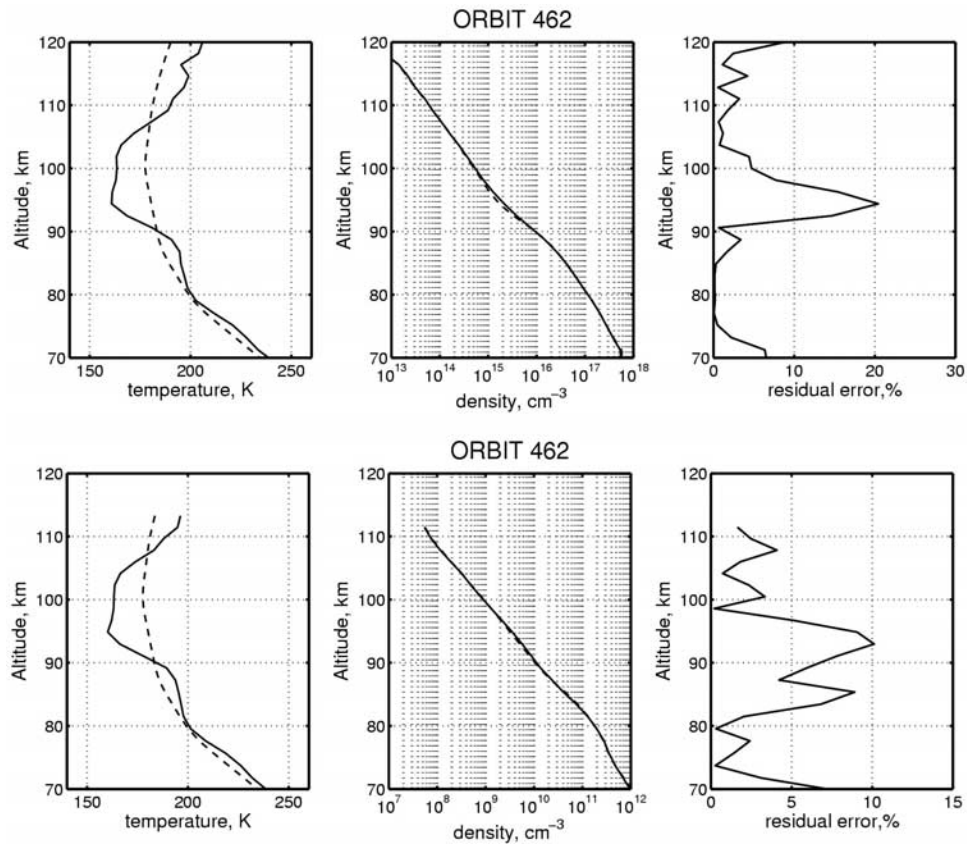


**Figure 8.** Sensitivity of the retrieved parameters to the temperature profile. The results are presented for retrieval of CO<sub>2</sub> (order 149, top) and H<sub>2</sub>O (order 171, bottom). They were obtained during orbit 462 (27 July 2007 at latitude 87.7°N, longitude 255°E, and 23.6 h LT, distance to the limb at altitude 80 km is around 1830 km). Left shows the temperature profiles used for the retrievals; middle shows the retrieved densities; right shows the residual error in % calculated as  $(N_1(z)-N_2(z))/N_1(z)$ , where  $N_1(z)$  and  $N_2(z)$  are the densities obtained for two different temperature profiles.

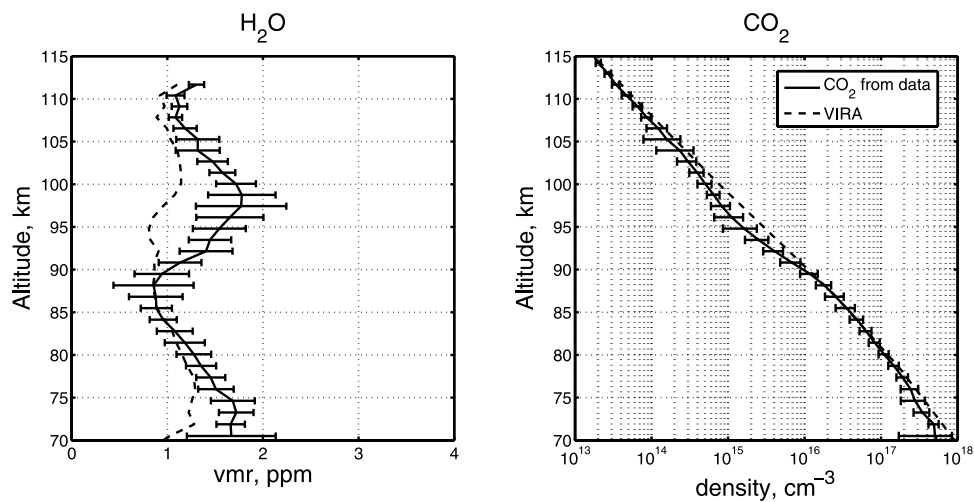


**Figure 9.** Comparison of the volume mixing ratios (vmr) of H<sub>2</sub>O using VIRA densities and CO<sub>2</sub> densities derived from measurements recorded on the same orbit. The example shows the results obtained for orbit 442 (7 July 2007, at latitude 79°N, longitude 284°E, and 20.7 h LT, distance to the limb at altitude 80 km is around 1780 km).

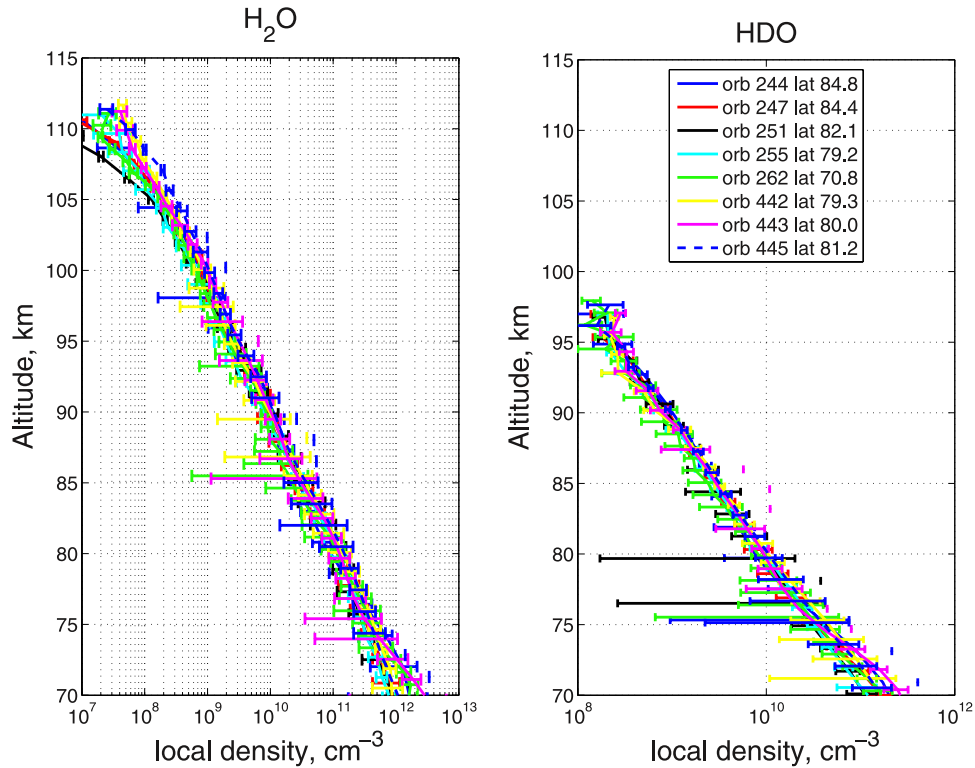


**Figure 10.** Vertical distributions of the H<sub>2</sub>O and HDO local density for eight orbits: five consecutive orbits from MTP09 (from 19 December 2006 to 10 January 2007) and three consecutive orbits from MTP016 (from 1 July 2007 to 27 July 2007), where MTP is the medium term plan. The conditions of observations are listed in Table 1.

profiles have been detected for the altitude range of 75–110 km. The latitude of observations varies for these orbits from 70° to 88°N. The mixing ratios of H<sub>2</sub>O and HDO for the same orbits are presented in Figure 11.

[39] A marked depletion of H<sub>2</sub>O is observed in the range 80–90 km, for which we have no explanation yet, other than noting that this altitude range coincides with the mesospheric minimum temperature and the top of the haze layer. The bump of H<sub>2</sub>O and HDO at 90–100 km relates to depletion of CO<sub>2</sub> density retrieved from CO<sub>2</sub> order. Figure 9 demonstrates the difference between mixing ratios obtained assuming CO<sub>2</sub> density from observations and from VIRI models. This depletion could be related to a strong temperature inversion with minimum at altitude ~85–90 km and we keep this study for a separate paper dedicated to the retrieval temperature and pressure profiles from CO<sub>2</sub> lines. The curves of both isotopes show little variability.

[40] The mean mixing ratio of H<sub>2</sub>O has been calculated for each orbit by averaging at altitudes from 75 to 112 km. The values are varying from 0.8 to 1.5 ppm. The temporal variation from orbit to orbit and the latitude variation of mixing ratios are presented in Figure 12. There is no systematic behavior in the distribution detected and the variations could reflect uncertainties of the SOIR observations. For HDO, mixing ratios were averaged from 75 to 95 km, the values varying from 50 to 130 ppb. Table 1 summarizes the averaged values of H<sub>2</sub>O and HDO volume mixing ratios (vmr). To make the comparison easier, the averaging of H<sub>2</sub>O for the same altitude range as HDO is

also presented in Table 1. The error bar corresponds to the error of the average in this case.

[41] The vertical distribution of D/H ratio can be easily obtained from H<sub>2</sub>O and HDO density profiles. The complete set of results is presented in Figure 13. There are some vertical variations of the isotopic ratio that have been discussed by *Bertaux et al.* [2007b]. The average isotopic ratios scaled to the standard mean ocean water (SMOW) ratio of  $3.10693 \times 10^{-4}$  and averaged at the range of altitudes from 75 to 90 km are shown in Figure 14 as a function of orbit number and latitude. The obtained values range between 200 and 300 times terrestrial with the average of  $240 \pm 25$ .

## 5. Discussion

[42] There were no continuous sets of H<sub>2</sub>O observations in the Venusian mesosphere before Venus Express. *Sandor and Clancy* [2005] and *Gurwell et al.* [2007] have made systematic observations of the mesosphere from ground-based and orbital telescopes. The summary of previous measurements is presented in Table 2. Most of the ground-based observations correspond to measurements of the Venusian disc and the direct comparison with the local observations of SOIR is not possible. Ground-based observations cannot directly resolve the vertical distribution of the species and inversion techniques are required to derive the profile from a single observation. The advantage of SOIR is that direct measurements of vertical profiles from the orbit are made possible. Moreover, simultaneous obser-

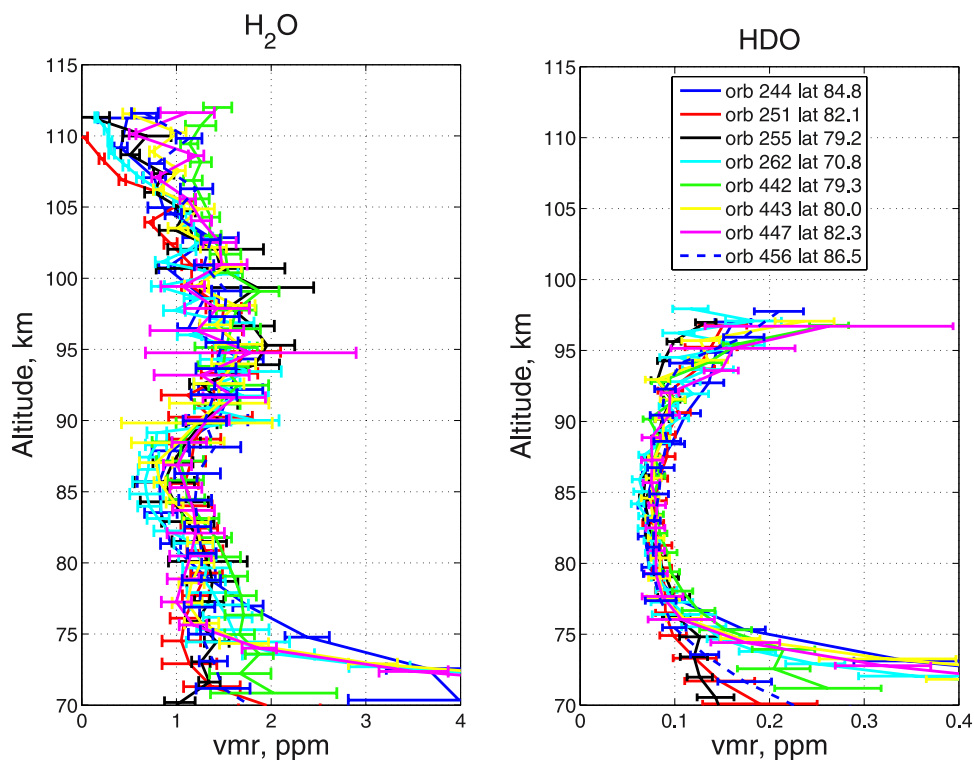


**Figure 11.** Vertical distributions of the H<sub>2</sub>O and HDO volume mixing ratios for eight orbits: four consecutive orbits from MTP09 and four consecutive orbits from MTP016. The conditions of observations are listed in Table 1.

variations in spectral ranges corresponding to both H<sub>2</sub>O and HDO are sometimes difficult to realize from the Earth. Several observations of H<sub>2</sub>O [Encrenaz *et al.*, 1991; Sandor and Clancy, 2005] are, in fact, measurements of HDO lines and rely on the HDO/H<sub>2</sub>O ratio obtained from other measurements. The volume mixing ratio of H<sub>2</sub>O (~1 ppm)

measured by SOIR is well consistent or lower than obtained from the Earth. The HDO mixing ratio of 0.08 ppm from SOIR is also lower than values obtained by Encrenaz *et al.* [1991, 1995] and by Sandor and Clancy [2005], but all values are in agreement within the error bars.

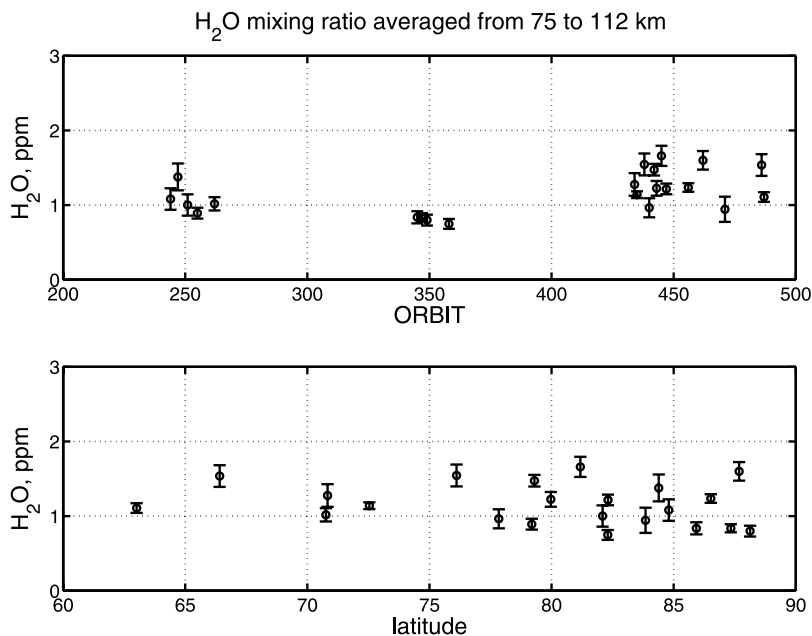


**Figure 12.** Temporal and latitudinal evolution of the H<sub>2</sub>O volume mixing ratios averaged as described in the text for orbits listed in Table 1. The H<sub>2</sub>O mixing ratio has been obtained by division by CO<sub>2</sub> densities from the same observations.

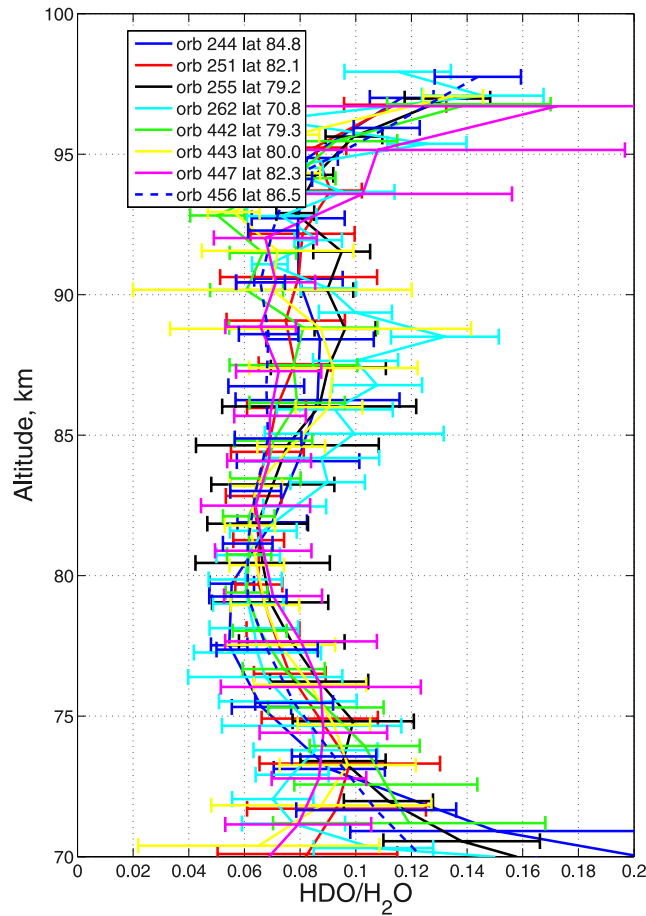


**Figure 13.** Vertical distributions of the HDO/H<sub>2</sub>O ratio for several orbits.

[43] High variability of H<sub>2</sub>O in the Venus mesosphere was recently detected by *Sandor and Clancy* [2005] and *Gurwell et al.* [2007]. This variability is not supported by SOIR observations at least near the north pole region. The

SOIR values show variations, but no more than a factor of 2 around the mean value (1 ppm), staying inside the SOIR uncertainties (except perhaps in the lowermost range 70–75 km, where errors are greater). But the direct compar-

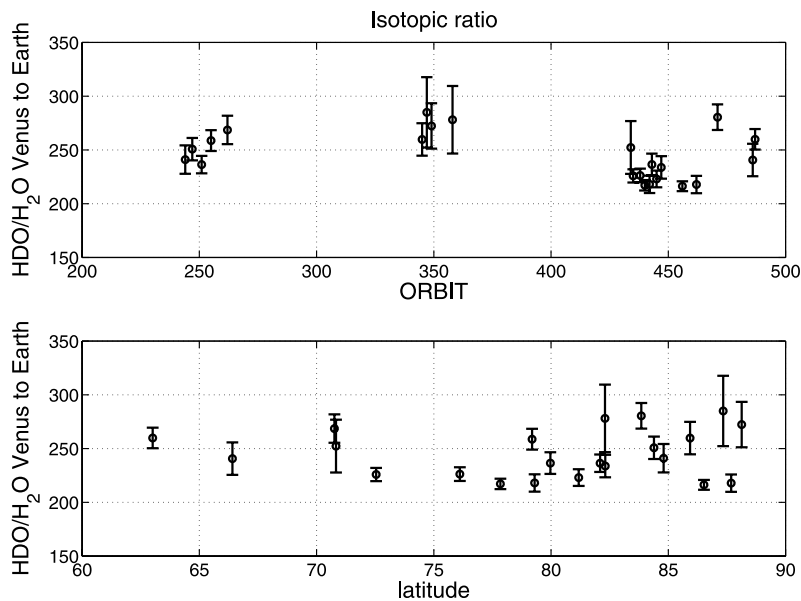


**Figure 14.** Temporal and latitudinal evolution of the HDO/H<sub>2</sub>O ratio scaled to Earth's value.

**Table 2.** Comparison of Averaged Values of the H<sub>2</sub>O and HDO Mixing Ratios With Previous Observations

Years	Altitude (km)	Spectral Range	H <sub>2</sub> O (ppm)	HDO (ppm)	Reference
1990	60–95	225.9GHz (HDO)	3.5 ± 2 (D/H = 120 terrestrial value)	0.13	<i>Encrenaz et al.</i> [1991]
1990–1993	60–95	187.31GHz (H <sub>2</sub> O) 225.9GHz (HDO)	1 ppm	0.26	<i>Encrenaz et al.</i> [1995]
1992?	72	2.59–2.65 μm (HDO and H <sub>2</sub> O)	2.09 ± 0.15	0.102	<i>Bjoraker et al.</i> [1992]
1998–2004	65–100	226 GHz (HDO) and 335 GHz	0 ± 0.06 3.5 ± 0.3	0 0.17	<i>Sandor and Clancy</i> [2005]
2002–2004	65–100	547.676GHz (H <sub>2</sub> O) and 556.936GHz	4.5 ± 1.5	-	<i>Gurwell et al.</i> [2007]
2006–2007	75–95	2.61 μm (H <sub>2</sub> O) 3.58 μm (HDO)	0.8–1.5	0.05–0.13	This research

ison with the ground-based observations is not possible. SOIR measures only morning or evening profiles at terminator, whereas values of H<sub>2</sub>O from millimeter observation may reflect disc averaged variability. It is equally difficult to compare our results to the H<sub>2</sub>O afternoon bulge observed by Pioneer Venus orbiter at the altitudes of 62–70 km in low and middle latitudes from 10°S to 60°N [*Koukouli et al.*, 2005]. Therefore, more SOIR occultations in wider latitude range are required to understand spatial variations of water vapor in the mesosphere.

[44] Several measurements of the D/H ratio in the Venus' mesosphere have already been performed before. The 2.3 μm window has been used to observe lines from both H<sub>2</sub>O and the deuterated water HDO and to measure the D/H ratio below the clouds from ground-based observations. *de Bergh et al.* [1991] derived a value of 120 ± 40 times the terrestrial SMOW value from high-resolution CFHT spectra on the nightside. *Donahue et al.* [1982, 1997] has reported the first determinations of the D/H ratio performed in situ by the neutral mass spectrometer of Pioneer Venus, the analysis of their data yields a value of D/H = 100 ± 12.5 corrected later to 157 ± 30 times the ratio in Earth's oceans. *Bjoraker et al.* [1992] have obtained the value of 157 ± 15 times terrestrial using near-IR dayside ground-based observations. The isotopic ratio retrieved from SOIR measurements (240 ± 25) times terrestrial is higher (factor ~1.5) than the results of all previous measurements in the lower atmosphere 157 ± 30 [*Donahue et al.*, 1997] and the measurements by *Bjoraker et al.* [1992] at the effective altitude of 72 km but they support the higher abundance of HDO to H<sub>2</sub>O compared to Earth.

[45] One motivation to HDO and H<sub>2</sub>O measurements in the upper atmosphere of Venus was to determine if HDO was present up to the altitude of photodissociation, providing D atoms for further escape. Clearly this D escape needs to be quantified, if we want to extrapolate back in time what was the original content of water on Venus. In the Earth's stratosphere, there is a cold trap at the tropopause, and preferential condensation of HDO versus H<sub>2</sub>O is an important factor of fractionation, which is circumvented by deuterated methane (CH<sub>3</sub>D) passing through the tropopause without condensing [*Moyer et al.*, 1996]. On Mars, the observed depletion of atomic D in the upper atmosphere [*Krasnopolsky et al.*, 1998] was explained by the lower HDO photolysis rate [*Cheng et al.*, 1999],

preferential condensation of HDO [*Fouchet and Lellouch*, 2000; *Bertaux and Montmessin*, 2001], and the smaller observed abundance of H<sub>2</sub> [*Krasnopolsky and Feldman*, 2001] than expected from models. Thermal and nonthermal escapes of D are weaker than those of H [*Krasnopolsky*, 2002] and tend to increase D/H.

[46] Our present results show that on Venus, there is no condensation of H<sub>2</sub>O nor HDO, and no cold trap preventing HDO to be photodissociated in the region above 80 km. On the contrary, one has to explain why the ratio HDO/H<sub>2</sub>O is found ≈1.5 times higher than lower in the atmosphere, with a possible trend of increasing with altitude (Figure 13). *Bertaux et al.* [2007b] proposed two explanations: the higher photodissociation rate of H<sub>2</sub>O [*Cheng et al.*, 1999] will preserve more HDO; also, if D atoms are not at all escaping at the top of the atmosphere, they may eventually recombine with OH radicals, generating a downward HDO flow, and further decrease the importance of HDO photodissociation. In any case, detailed modeling of these mechanisms is necessary, but it is beyond the scope of the present paper.

## 6. Conclusions

[47] We report vertical distributions of the molecular density and mixing ratios of H<sub>2</sub>O and HDO in the Venus mesosphere by SOIR, a high-resolution (with R~20,000) echelle spectrometer on board Venus Express. The spectrometer operates in solar occultation mode and sounds the atmosphere at the range of altitudes from 65 to 130 km. Simultaneous measurements of water vapor lines in the 2.61 μm range (3830 cm<sup>-1</sup>) at altitudes of 70–110 km and HDO lines in the 3.58 μm range (2715 cm<sup>-1</sup>) at altitudes of 70–95 km have been performed. For a year and a half, from April 2006 to August 2007, 54 such measurements have been carried out at different locations on Venus from the north pole to middle south latitudes mainly in the high northern latitudes at the morning and evening terminator. After in-flight recalibration of the spectrometer during summer 2007, a new analysis of the observed H<sub>2</sub>O has been undertaken. We analyzed the mixing ratio and isotopic values obtained from 22 orbits corresponding to high northern latitudes. The temporal variations have been investigated. The averaged volume mixing ratios of H<sub>2</sub>O = 1.16 ± 0.24 ppm and HDO = 0.086 ± 0.020 ppm have been obtained for this set of orbits. The depletion in the mixing ratios of H<sub>2</sub>O and HDO near 85 km is related to the

depletion in the CO<sub>2</sub> density near 95 km and a possible temperature inversion at these altitudes. No large variability of H<sub>2</sub>O has been detected for the high northern latitudes observations. The time variation of the mixing ratios of HDO and H<sub>2</sub>O do not exceed 2–3 times the mean value. The obtained HDO/H<sub>2</sub>O ratio equals  $240 \pm 25$  times the ratio in the Earth' ocean on the average, which is higher than previously reported values by a factor  $\sim 1.5$ .

[48] Future analysis of SOIR data corresponding to middle and lower latitudes of Venus and to a wider set of observations will allow understanding the possible long-term variations. We also count on more accurate instrumental calibration and improved simultaneously retrieval of temperature from SOIR data.

[49] The resulting vertical profiles of water vapor and its isotopologue could give an exciting challenge to the development of new photochemical models of the upper atmosphere of Venus. Such investigations have already started with models such the one developed by M.-C. Liang and Y. L. Yung (Modeling the distribution of H<sub>2</sub>O and HDO in the upper atmosphere of Venus, submitted to *Journal of Geophysical Research*, 2008). Moreover, combination of VIRTIS and SPICAV nadir measurements of H<sub>2</sub>O below and above the clouds could reconstruct a global distribution of water vapor in the Venus atmosphere [Drossart et al., 2007; Bertaux et al., 2007a; Marcq et al., 2008].

[50] These profiles give also hints to estimation of past and present escape from the planet. If there were no escape of D atoms, now and in the past, the present 1 cm (equivalent liquid) and D/H ratio  $\approx 0.025$  (enrichment 150) would imply in the past only 1.5 m, compared to 2.8 km on Earth. With the present observation of plenty of HDO in the photodissociation region, D atoms are certainly present in the thermosphere. It would be important to quantify the escape of D atoms, possibly by measuring mass 2 ions escape as could do ASPERA on board Venus Express [Barabash et al., 2007]. In spite of the possible confusion with H<sub>2</sub><sup>+</sup> ions, it would provide a useful upper limit to D<sup>+</sup> ion escape [McElroy et al., 1982; Hartle and Taylor, 1983].

[51] **Acknowledgments.** We would like to thank our reviewers for helpful comments that improved the manuscript. We thank our collaborators at the three institutes for the design and fabrication of the SOIR instrument, which was mainly built in Belgium by OIP company, under the direction of IASB-BIRA. Russian team acknowledges RFBR grant 06-02-72563. Belgium team was supported by the Belgian Federal Science Policy Office and the European Space Agency (ESA, PRODEX program, contracts C 90268, 90113, and 17645). Procurement of AOTF was funded by CNES and the French authors are sponsored by CNRS and CNES. We thank A. Bensoussan (COB) for procuring in due time the SOFRADIR detector.

## References

- Barabash, S., et al. (2007), The analyser of space plasmas and energetic atoms (ASPERA-4) for the Venus Express mission, *Planet. Space Sci.*, **55**, 1772–1792.
- Bertaux, J. L., and F. Montmessin (2001), Isotopic fractionation through water vapor condensation: The Deuteropause, a cold trap for deuterium in the atmosphere of Mars, *J. Geophys. Res.*, **106**(E12), 32,879–32,884, doi:10.1029/2000JE001358.
- Bertaux, J.-L., et al. (2007a), SPICAV on Venus Express: Three spectrometers to study the global structure and composition of the Venus atmosphere, *Planet. Space Sci.*, **55**, 1673–1700, doi:10.1016/j.pss.2007.01.016.
- Bertaux, J.-L., et al. (2007b), A warm layer in Venus' cryosphere and high altitude measurements of HF, HCl, H<sub>2</sub>O and HDO, *Nature*, **450**, 646–649, doi:10.1038/nature05974.
- Bjoraker, G. L., H. P. Larson, M. J. Mumma, R. Timmermann, and J. L. Montani (1992), Airborne observations of the gas composition of Venus above the cloud tops: Measurements of H<sub>2</sub>O, HDO, HF, and the D/H and <sup>18</sup>O/<sup>16</sup>O isotopic ratios, *Bull. Am. Astron. Soc.*, **24**, 995.
- Brown, L. R., C. M. Humphrey, and R. R. Gamache (2007), CO<sub>2</sub>-broadened water in the pure rotation and n<sub>2</sub> fundamental regions, *J. Mol. Spectrosc.*, **246**, 1–21, doi:10.1016/j.jms.2007.07.010.
- Cheng, B.-M., E. P. Chew, C.-P. Liu, M. Bahou, Y.-P. Lee, Y. K. Yung, and M. F. Gerstell (1999), Photo-induced fractionation of water isotopomers in the Martian atmosphere, *Geophys. Res. Lett.*, **26**(24), 3657–3660, doi:10.1029/1999GL008367.
- de Bergh, C., B. Bezard, T. Owen, D. Crisp, J.-P. Maillard, and B. L. Lutz (1991), Deuterium on Venus: Observations from Earth, *Science*, **251**, 547–549.
- de Bergh, C., V. I. Moroz, F. W. Taylor, D. Crisp, B. Bézard, and L. V. Zasova (2006), Composition of the atmosphere of Venus below the clouds, *Planet. Space Sci.*, **54**, 1389–1397.
- Donahue, T. M., J. H. Hoffman, R. R. Hodges, and A. J. Watson (1982), Venus was wet: A measurement of the ratio of deuterium to hydrogen, *Science*, **216**, 630–633.
- Donahue, T. M., D. H. Grinspoon, R. E. Hartle, and R. R. Hodges Jr. (1997), Ion/neutral escape of hydrogen and deuterium: Evolution of water, in *Venus II: Geology, Geophysics, Atmosphere, and Solar Wind Environment*, edited by Stephen W. Bougher et al., pp. 385–415, Univ. of Ariz. Press, Tucson.
- Drossart, P., et al. (2007), Scientific goals for the observation of Venus by VIRTIS on ESA/Venus Express mission, *Planet. Space Sci.*, **55**, 1653–1672, doi:10.1016/j.pss.2007.01.003.
- Encrenaz, T., E. Lellouch, G. Paubert, and S. Gulkis (1991), First detection of HDO in the atmosphere of Venus at radio wavelengths: An estimate of the H<sub>2</sub>O vertical distribution, *Astron. Astrophys.*, **246**(1), L63–L66.
- Encrenaz, T. H., E. Lellouch, J. Cernicharo, G. Paubert, S. Gulkis, and T. Spilker (1995), The thermal profile and water abundance in the Venus mesosphere from H<sub>2</sub>O and HDO millimeter observations, *Icarus*, **117**, 162–172, doi:10.1006/icar.1995.1149.
- Fouchet, T., and E. Lellouch (2000), Vapor pressure isotope fractionation effects in planetary atmospheres: Application to deuterium, *Icarus*, **144**, 114–123, doi:10.1006/icar.1999.6264.
- Gamache, R. R., S. P. Neshyba, J. J. Planeaux, A. Barbe, L. Regalia, and J. B. Pollack (1995), CO<sub>2</sub>-broadening of water vapor lines, *J. Mol. Spectrosc.*, **170**, 131–151, doi:10.1006/jmsp.1995.1060.
- Gurwell, M. A., G. J. Melnick, V. Tolls, E. A. Bergin, and B. M. Patten (2007), SWAS observations of water vapor in the Venus mesosphere, *Icarus*, **188**, 288–304.
- Hagemann, R., G. Nief, and E. Roth (1970), Absolute isotopic scale for deuterium analysis in natural waters: Absolute D/H ratio of SMOW, *Tellus*, **22**, 712–715.
- Hartle, R. E., and H. A. Taylor (1983), Identification of deuterium ions in the ionosphere of Venus, *Geophys. Res. Lett.*, **10**(10), 965–968, doi:10.1029/GL010i010p00965.
- Howard, T. N., D. E. Burch, and D. Willams (1956a), Infrared transmission of synthetic atmospheres: 1. Instrumentation, *J. Opt. Soc. Am.*, **46**, 186–190.
- Howard, T. N., D. E. Burch, and D. Willams (1956b), Infrared transmission of synthetic atmospheres: 2. Absorption by carbon dioxide, *J. Opt. Soc. Am.*, **46**, 237–241.
- Howard, T. N., D. E. Burch, and D. Willams (1956c), Infrared transmission of synthetic atmospheres: 3. Absorption by water vapor, *J. Opt. Soc. Am.*, **46**, 242–245.
- Howard, T. N., D. E. Burch, and D. Willams (1956d), Infrared transmission of synthetic atmospheres: 4. Application of theoretical band models, *J. Opt. Soc. Am.*, **46**, 334–338.
- Keating, G. M., et al. (1985), VIRA (Venus International Reference Atmosphere) models of Venus neutral upper atmosphere: Structure and composition, *Adv. Space Res.*, **5**(11), 117–171.
- Korablev, O., and J.-L. Bertaux (2002), Soir experiment for Venus Express: Scientific objectives for solar occultations, paper presented at XXVII General Assembly, Eur. Geophys. Soc., Nice, France, 21–26 April 2002, Abstract 3506.
- Koukoulis, M. E., P. G. J. Irwin, and R. W. Taylor (2005), Water vapor abundance in Venus' middle atmosphere from Pioneer Venus OIR and Venera 15 FTS measurements, *Icarus*, **173**, 84–99, doi:10.1016/j.icarus.2004.08.023.
- Krasnopolsky, V. A. (2002), Mars' upper atmosphere and ionosphere at low, medium, and high solar activities: Implications for evolution of water, *J. Geophys. Res.*, **107**(E12), 5128, doi:10.1029/2001JE001809.

- Krasnopolsky, V. A., and P. D. Feldman (2001), Detection of molecular hydrogen in the atmosphere of Mars, *Science*, *294*, 1914–1917, doi:10.1126/science.1065569.
- Krasnopolsky, V. A., M. J. Mumma, and G. R. Gladstone (1998), Detection of atomic deuterium in the upper atmosphere of Mars, *Science*, *280*, 1576–1580, doi:10.1126/science.280.5369.1576.
- Mahieux, A., et al. (2008), In-flight performance and calibration of SPICAV SOIR on board Venus Express, *Appl. Opt.*, *47*, 2252–2265, doi:10.1364/AO.47.002252.
- Marcq, E., et al. (2008), A latitudinal survey of CO, OCS, H<sub>2</sub>O and SO<sub>2</sub> in the lower atmosphere of Venus: Spectroscopic studies using VIRTIS-H, *J. Geophys. Res.*, *113*, E00B07, doi:10.1029/2008JE003074.
- McElroy, M. B., M. J. Prather, and J. M. Rodriguez (1982), Escape of hydrogen from Venus, *Science*, *215*, 1614–1615, doi:10.1126/science.215.4540.1614.
- Moyer, E. J., F. W. Irion, Y. L. Yung, and M. R. Gunson (1996), ATMOS stratospheric deuterated water and implications for troposphere-stratosphere transport, *Geophys. Res. Lett.*, *23*(17), 2385–2388, doi:10.1029/96GL01489.
- Nevejans, D., et al. (2006), Compact high-resolution space-borne echelle grating spectrometer with AOTF based order sorting for the infrared domain from 2.2 to 4.3 micrometer, *Appl. Opt.*, *45*, 5191–5206, doi:10.1364/AO.45.005191.
- Pollack, J. B., et al. (1993), Near-infrared light from Venus' nightside: A spectroscopic analysis, *Icarus*, *103*, 1–42.
- Press, W. H., B. P. Flannery, S. A. Teukolsky, and W. T. Vetterling (1992), Numerical Recipes in *FORTRAN: The Art of Scientific Computing*, 2nd ed., 992 pp., Cambridge Univ. Press, Cambridge, U. K.
- Rodgers, C. D. (2000), *Inverse Methods for Atmospheric Sounding: Theory and Practice. Atmos., Oceanic Planet. Phys. Ser.*, vol. 2, World Sci., Hackensack, N. J.
- Rothman, L. S., et al. (2005), The HITRAN 2004 molecular spectroscopic database, *J. Quant. Spectrosc. Radiat. Transfer*, *96*, 139–204, doi:10.1016/j.jqsrt.2004.10.008.
- Sandor, B. J., and R. T. Clancy (2005), Water vapor variations in the Venus mesosphere from microwave spectra, *Icarus*, *177*, 129–143.
- Titov, D. V., et al. (2006), Venus Express science planning, *Planet. Space Sci.*, *54*, 1279–1297, doi:10.1016/j.pss.2006.04.017.
- Vandaele, A. C., et al. (2008), Composition of the Venus mesosphere measured by SOIR on board Venus Express, *J. Geophys. Res.*, doi:10.1029/2008JE003140, in press.
- 
- D. Belyaev, A. Fedorova, and O. Korablev, Space Research Institute, 117997, 84/32 Profsoyuznaya Street, Moscow, Russia. (fedorova@irn.iki.rssi.ru)
- J.-L. Bertaux, F. Montmessin, and E. Villard, Service d'Aéronomie du CNRS, BP 3, F-91371, Verrières-le-Buisson, France.
- R. Drummond, A. Mahieux, E. Neefs, A.-C. Vandaele, and W. V. Wilquet, Belgian Institute for Space Aeronomy, 3 avenue Circulaire, B-1180 Brussels, Belgium.